Cooperative Marine Vehicle Navigation and Control with Applications to Geotechnical Surveying

Francisco Branco
francisco.branco@tecnico.ulisboa.pt

Instituto Superior Técnico, Lisboa, Portugal

June 2022

Abstract

Marine environments bear challenging conditions for humans, thus making it very difficult to explore thoroughly these areas. Seismic surveying is one of the activities engaged regarding marine exploration, usually performed with the help of large vessels towing massive grids of acoustic antennas. This work proposes a separation of the acoustic source and the antennas using a network of Autonomous Marine Vehicles (AMVs), where a system with multiple layers of cooperation allows for an enhanced capture of seismic data. The designed system yields two groups of vehicles, a group of Autonomous Underwater Vehicles (AUVs) which perform a simple Cooperative Path Following (CPF) technique over a desired path, and a group of Autonomous Surface Vehicles (ASVs) which in turn perform an encircling manoeuvre around the group of AUVs, using a Moving Path Following (MPF) approach. The Final layer of Cooperative Multiple Formation Control (CFMC) is formed between the two groups of vehicles, taking into account delays on the overall coordination. A filter application is also implemented to help the AUV underwater localisation.
Keywords: Autonomous Marine Vehicles, Cooperative Path Following, Moving Path, Vehicle Estimation, Cooperation of Multiple Formations

1. Introduction

Cooperative Marine Vehicle Control has turned into a very attractive topic of research since it has been the inspiration for many projects within both the academy and industry environments. When it comes to the use of AMVs for geotechnical surveys, the typical formations of deployed cooperative vehicles are purposefully designed in order to increase the overall accuracy and precision of the survey. However, the approach developed in this thesis brings a new perspective to the existing standards. The end goal is to have ASVs encircling the submerged centre of mass of a group of AUVs (supposedly towing acoustic antennas or, in other words, streamers), and following this circular motion. The premise to justify this logic comes from geophysical studies in the field of seismic reflection surveying. By dividing the ocean floor in cells, it was noticed that when each cell was hit by acoustic waves from different angles, the accuracy of the mapping was substantially increased, making it possible to derive an acoustic impedance from each cell at different depths [1]. Following this line of thought, by having multiple ASVs acting as acoustic sources while circulating the AUVs carrying the streamers, hitting the ocean floor with acoustic waves, the latter can pick up the waves that ricochet off each cell at different depths, gaining an overall better resolution on the mapping of the seabed layers.

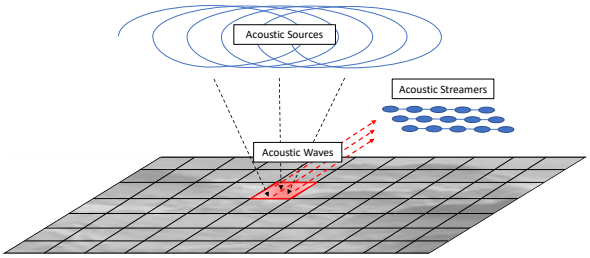

Figure 1: Illustration of the proposed system.

1.1. State of the Art

After describing the general problem, one must become familiar with the technical aspects of the problem. The project is divided into many sub-problems to simplify its development. The first issue to be addressed is Path Following (PF), a control method which outputs a law for vehicles to converge to a desired path. In order to achieve the goals established for this project, the algorithm described in

Lapierre et al. [2] was used for the general PF technique of the system. This method is very useful since it gives direct access to virtual target on the path which the vehicle converge to, serving as a path parameterisation for future usage. Not only that, but it also presents global convergence to the path as time tends to infinity.

Secondly, there is the problem of CPF, where AMVs cooperate to converge to a path in a coordinated formation. The CPF basic structure is described in Ghabcheloo et al. [3], where a coordinated state is derived from a normalised path parameterisation, and a velocity control law is defined to achieve coordination. Another problem arises when one takes into account the discrete nature of these transmissions to establish cooperation between AMVs, as well as the low-bandwidth of the water column for acoustic communications. This is where Event-Triggered Communications (ETC) come into play, addressing both these issues and equipping the AMVs with a way to communicate more scarcely. The discrete CPF and ETC mechanisms are carefully depicted in Rego et al. [4] and Hung et al. [5].

The circular motion necessary for each ASV tracker is obtained implementing an MPF technique around a certain target. The strategy was proposed in Oliveira et al. [6] for aerial vehicles, and adapted in Teixeira [7] for AMVs. The control mechanism computes a law for the new desired velocity and heading of each vehicle, which need to compensate for the moving target.

A filter application was also tackled, in order to find an estimate for the target to encircle and to equip the target with a better vehicle localisation when considering the real case. Therefore, an Extended Kalman Filter (EKF) was implemented on one of the ASV trackers, for the target estimation, resorting to range-measurements between the ASVs and the AUVs, and a Complementary Kalman Filter (CKF) to help the localisation problem on the AUVs, which in turn receives the EKF estimation from the ASV trackers and blends it with the Doppler Velocity Log (DVL) velocity measurements within the AUV. The EKF was based on the work developed in Hung et al. [8], and the CKF took inspiration from the Complementary Filters approach in [9], later converting the filter into a CKF with time-varying gains.

Finally, the designed Cooperative Multiple Formation Control (CMFC) mechanism took great influence from the previous work in Teixeira [7], effectively creating a cooperation layer between different groups of AMVs. The Cooperative Multiple Formation Control is a novel solution to this problem, and is heavily based on CPF techniques. The velocity control law of Smart Cooperative Path Following (SCPF) was also defined for every vehicle, to achieve a better approximation to the path before starting to coordinate their states, i.e., to perform the PF until the vehicle gets close enough to the path and start employing the CPF technique.

2. Problem Statement

In order to simplify the study and testing of the techniques employed in this work, the vehicle model only regarded the kinematics, defined as

$$\begin{cases} \dot{x} &= v \cdot \cos\theta\,, \\ \dot{y} &= v \cdot \sin\theta\,, \\ \dot{\theta}_m &= \omega_m\,, \end{cases} \tag{1}$$

where the velocity v and angle rate ω_m are inputs to be controlled so that path convergence and vehicle coordination is achieved. It is also assumed the sideslip is negligible, i.e., the angle $\beta = 0$. The final system is endowed with the capability of performing a cooperation strategy between the ASV formation $\mathcal{F}_{ASV}$ and the AUV formation $\mathcal{F}_{AUV}$, controlling the velocity v and angle rate ω_m of each vehicle in both formations, converging the vehicles to their respective paths while achieving a certain formation by coordinating between each other as $t \to \infty$. According to the vehicle model in (1), and to simplify the problem at hand, it is assumed the vehicles move in the same 2D plane, regardless of being AUVs or ASVs. The communications between vehicles in $\mathcal{F}_{ASV}$ is considered trivial, since it can be performed over Wi-Fi connection. On the other hand, communications between vehicles from $\mathcal{F}_{ASV}$ and $\mathcal{F}_{AUV}$ must take place through the acoustic channel, hence taking into account the constraints imposed by this type of communications. Between vehicles within the same formation $\mathcal{F}_{AUV}$, the communications must be through the acoustic channel as well.

3. System Overview

The system is broken down into different parts for easier analysis. The basic block of the entire system is the PF strategy. The remaining concepts are sequentially implemented on top of it.

3.1. Path Following

The chosen PF mechanism follows the work in [2], where an approach was presented using a path parameterisation of $\boldsymbol{p} : s \to [x, y]$ for a certain path. The algorithm consists of creating a virtual target projected directly on the desired path, which in turn is pursued by the vehicle itself. The angle rate $\dot{\theta}_m$ of the vehicle is then controlled to make the vehicle converge to the path. The model for the virtual target P is given as

$$\begin{cases} \dot{s}_1 &= -\dot{s}(1 - c_c \cdot y_1) + v \cdot cos\theta\,, \\ \dot{y}_1 &= -c_c \cdot \dot{s} \cdot s_1 + v \cdot sin\theta\,, \\ \dot{\theta} &= \omega_m - c_c \cdot \dot{s}\,, \end{cases} \tag{2}$$

where (s_1, y_1) are the $(x_{\mathcal{SF}}, y_{\mathcal{SF}})$ components of the position of the vehicle in the *Serret-Frenet* frame $\{\mathcal{SF}\}$ placed on the virtual target, as it can be seen in Figure 2. The angle θ is calculated as $\theta = \theta_m - \theta_c$, with θ_c being the tangential angle of the virtual target's point in the path P.

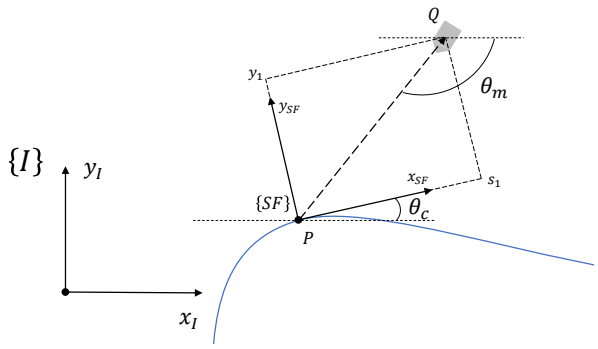

Figure 2: Path Following problem.

To achieve convergence, (s_1, y_1) must be driven to zero as time tends to infinity. Thus, the control law proposed in [2] is defined as

$$\begin{cases} \dot{s} & = v \cdot cos\theta + k_1 \cdot s_1 \,, \\ \dot{\theta} & = \dot{\delta} - \gamma \cdot y_1 \cdot v \cdot \frac{sin\theta - sin\delta}{\theta - \delta} - k_2 \cdot (\theta - \delta) \,, \end{cases} \tag{3}$$

where s determines the position of the virtual target P on the path, and δ is a function designed to draw the vehicle to the path before converging its yaw θ_m to the desired tangential angle θ_c. The variables k_1, k_2 and γ are positive gains which need to be tuned. The final control law, revisiting the vehicle model in (1), is determined as

$$\dot{\theta}_m = \omega_m = \dot{\theta} + c_c \cdot \dot{s} \,. \tag{4}$$

As stated in [2], the algorithm presents global convergence as long as the vehicle presents a velocity profile $v_p > 0$. Another advantage of this algorithm is that, because of its parameterisation, the virtual target s can be used in the following subsystems.

3.2. Cooperative Path Following

CPF is a technique used on top of the PF to coordinate different vehicles on their respective paths. This approach is explained in [3]. A coordination state on vehicle i for a path p is then defined as

$$\gamma^{[i]}(t) = \frac{s^{[i]}(t)}{L_p} \,, \tag{5}$$

where L_p is the total path length, therefore corresponding to a normalisation of the variable s discussed in the previous section. Let $\mathcal{N}_i$ be a group of neighbouring vehicles to vehicle i in a network. Borrowing some concepts from Graph Theory as it is demonstrated in [10], the communications between vehicles are characterised by the normalised Laplacian $\boldsymbol{L}_D = \boldsymbol{D}^{-1}(\boldsymbol{D} - \boldsymbol{A})$, where $\boldsymbol{A}$ is the adjacency matrix and $\boldsymbol{D}$ is the degree matrix. An error between coordination states is introduced as

$$\boldsymbol{\epsilon} = \boldsymbol{L}_D \cdot \boldsymbol{\gamma} \,. \tag{6}$$

However, the communications in underwater environments have challenging constraints imposed on them, hence they are not time-continuous at all. A discretisation of the error is then considered as

$$\boldsymbol{\epsilon} = \boldsymbol{\gamma} - (\boldsymbol{D}^{-1} \cdot \boldsymbol{A})\hat{\boldsymbol{\gamma}} \,, \tag{7}$$

where $\hat{\boldsymbol{\gamma}}$ is a prediction of the coordination state of other vehicles. A control law for the desired velocity of each vehicle i can now be formulated as

$$v_d^{[i]} = v_p^{[i]} + v_c^{[i]} \,, \tag{8}$$

where $v_p^{[i]}$ is the velocity profile assigned to the vehicle i, and $v_c^{[i]}$ is a correction computed as

$$v_c^{[i]} = -k_\xi^{[i]} \cdot \tanh\left(\gamma_i^{[i]} - \frac{1}{|\mathcal{N}_i|} \sum_{j \in \mathcal{N}_i} \hat{\gamma}_j^{[i]} \right) \,, \tag{9}$$

where $k_\xi^{[i]}$ is a positive gain, γ_i is the real coordination state of vehicle i, and $\hat{\gamma}_j$ is the predicted coordination state of a neighbour vehicle j.

3.3. Event-Triggered Communications

In order to handle the communications underwater and to minimise the flow of messages between vehicles, the topic of ETC is introduced. The method used is detailed in [4] and [5], proposing a triggering function that dictates when there should be exchange of messages between vehicles. Two functions are available, a time-dependent and a state-dependent, depending on the mission at hand. For this work, the time-dependent function was chosen, triggering the vehicle to broadcast its state and estimates when the function $h^{[i]}(t) > 0$, which is given as

$$\begin{cases} h^{[i]}(t) & = |e^{[i]}(t)| - \eta^{[i]}(t) \,, \\ \eta^{[i]}(t) & = c_0 + c_1 \cdot e^{-c_2 \cdot t} \,, \end{cases} \tag{10}$$

where c_0, c_1 and c_2 are positive gains, and the error $e^{[i]}(t)$ is defined as

$$e^{[i]}(t) = \hat{\gamma}_i^{[i]} - \gamma_i^{[i]}(t) \,, \tag{11}$$

where γ_i is the actual vehicle i coordination state and $\hat{\gamma}_i$ is the self predicted coordination state. The vehicle i estimators are then modelled as

$$\begin{cases} \dot{\hat{\gamma}}_i^{[i]} & = v_p^i / L_i \,, \\ \dot{\hat{\gamma}}_j^{[i]} & = v_p^j / L_j \,, \end{cases} \tag{12}$$

where v_p is the velocity profile assigned to each vehicle, L is the total path length. The estimators have two more other properties, as the self estimator $\hat{\gamma}_i$ of vehicle i resets every time t_k there is a broadcast, and the estimators γ_j reset their values every time t_k there is a message reception from another neighbour vehicle $j \in \mathcal{N}_i$ to vehicle i. The described actions can be defined as

$$\begin{aligned} \hat{\gamma}_i^{[i]}(t_k^t) &= \gamma_i^{[i]}(t_k^t)\,, \\ \hat{\gamma}_j^{[i]}(t_k^r) &= \gamma_j^{[j]}(t_k^r)\,, \end{aligned} \tag{13}$$

where the time t_k^t is respective to the moment the function in (10) triggers and the vehicle i broadcasts its state to others, and the time t_k^r is respective to the moment the vehicle receives a broadcast from a neighbour vehicle j.
The topology of the CPF/ETC vehicle network can be verified in Figure 3. To the purpose of this work, it is considered that the derivative of the desired velocity $\dot{v}_d = 0$.

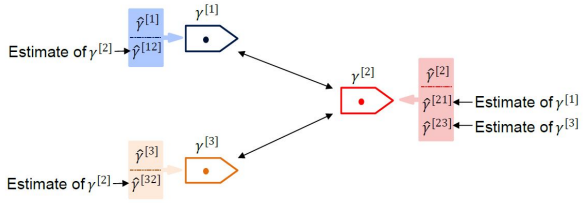

Figure 3: Vehicle network topology.[4]

3.4. Moving Path Following

The MPF method used is demonstrated in [6] for aerial vehicles, whereas in [7] a simpler approach was devised in the context of AMVs. With the previously explained strategies of PF and CPF, it was possible to have different groups of vehicles working together to make each vehicle follow a path in a coordinated manner. However, in order to achieve the group of ASV trackers encircling the AUV targets, the MPF subsystem must be implemented. In light of this, taking the outputs of the PF and CPF, it is possible to compute a new velocity and yaw angle for the trackers to follow.
To this end, a new reference frame $\mathcal{P}$ along with a circular path is projected on top of the moving target, as it is observed in Figure 4. In the scope of this project, it is considered that the moving path suffers merely a translation, since the rotation of the path is not necessary for the final system.

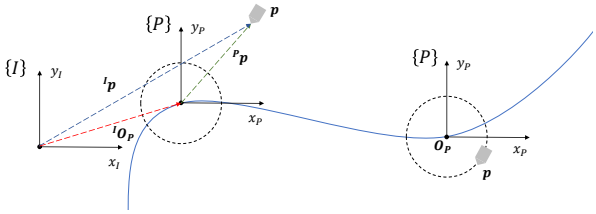

Figure 4: Moving Path Following problem.

The tracker's position represented in the inertial frame $\{\mathcal{I}\}$ is given as

$${}^{I}\boldsymbol{p} = {}^{I}\boldsymbol{O}_p + {}^{P}\boldsymbol{p}\,, \tag{14}$$

where ${}^{I}\boldsymbol{O}_p$ is the origin of the reference frame $\{\mathcal{P}\}$ placed on top of the target in the inertial frame $\{\mathcal{I}\}$, and ${}^{P}\boldsymbol{p}$ is the vehicle's position represented in the reference frame $\{\mathcal{P}\}$. The inertial velocity law can then be defined as

$${}^{\mathcal{I}}\dot{\boldsymbol{p}} = {}^{\mathcal{I}}\boldsymbol{v}_P + {}^{\mathcal{P}}\boldsymbol{v}\,, \tag{15}$$

where ${}^{\mathcal{I}}\boldsymbol{v}_P$ is the velocity of the target in the inertial frame $\{\mathcal{I}\}$, and ${}^{\mathcal{P}}\boldsymbol{v}$ is the velocity of the tracker in the reference frame $\{\mathcal{P}\}$. The resulting inertial velocity law is a vector of components x, y, from which can be deduced the desired velocity and yaw angle for the tracker that is performing the encircling manoeuvre around the targets. The resulting system for the ASV trackers can hence be described by the block diagram in Figure 5.

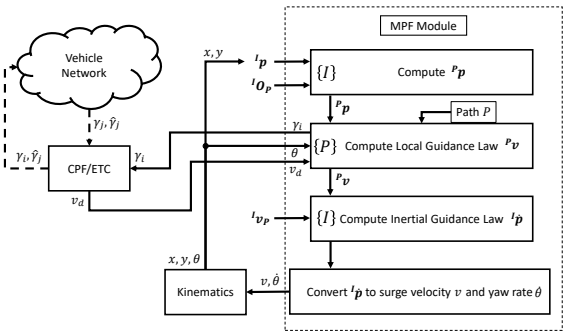

Figure 5: Moving Path Following problem.

3.5. Extended Kalman Filter

To bring the system closer to the real case, an EKF was implemented in the trackers performing the encircling manoeuvre, thus estimating the targets position and velocity. The filter used is clearly exposed in [8], with a linear prediction stage and a nonlinear update stage. The state to be predicted is expressed as $\boldsymbol{x} = [x, y, v_x, v_y]^T$. The prediction stage is then defined as

$$\begin{cases} \hat{\boldsymbol{x}}_{k|k-1} = \boldsymbol{F} \cdot \hat{\boldsymbol{x}}_{k-1|k-1}\,, \\ \boldsymbol{P}_{k|k-1} = \boldsymbol{F} \cdot \boldsymbol{P}_{k-1|k-1} \cdot \boldsymbol{F}^T + \boldsymbol{Q}\,, \end{cases} \tag{16}$$

where $\hat{\boldsymbol{x}}_{k-1|k-1}$ is the state estimate before the prediction, $\hat{\boldsymbol{x}}_{k|k-1}$ is the state estimate after the prediction, $\boldsymbol{P}_{k-1|k-1}$ is the probability matrix before the prediction, and $\boldsymbol{P}_{k|k-1}$ is the probability matrix after the prediction. The matrix $\boldsymbol{F}$ represents the process and is given as

$$\boldsymbol{F} = \begin{bmatrix} \boldsymbol{I}_2 & T_s \cdot \boldsymbol{I}_2 \\ \boldsymbol{0} & \boldsymbol{I}_2 \end{bmatrix}, \tag{17}$$

where T_s is the sampling period of the simulation. The matrix $\boldsymbol{Q}$ from (16) is the variance related to the process noise $\boldsymbol{\omega}_k \sim \mathcal{N}(0, \boldsymbol{Q})$. Next, the update stage is executed, and it is formulated as

$$\begin{cases} d_k(\hat{\boldsymbol{x}}_{k|k-1}) = ||\hat{\boldsymbol{p}} - \boldsymbol{q}||\,, \\ \boldsymbol{C}_k = \frac{d}{d\boldsymbol{x}} d_k(\hat{\boldsymbol{x}}_{k|k-1})\,, \\ \boldsymbol{K}_k = \boldsymbol{P}_{k|k-1} \cdot \boldsymbol{C}_k^T (\boldsymbol{C}_k \cdot \boldsymbol{P}_{k|k-1} \cdot \boldsymbol{C}_k^T + R)^{-1}\,, \\ \hat{\boldsymbol{x}}_{k|k} = \hat{\boldsymbol{x}}_{k|k-1} + \boldsymbol{K}_k (y_k - d_k(\hat{\boldsymbol{x}}_{k|k-1}))\,, \\ \boldsymbol{P}_{k|k} = (\boldsymbol{I}_4 - \boldsymbol{K}_k \cdot \boldsymbol{C}_k) \cdot \boldsymbol{P}_{k|k-1}\,, \end{cases} \tag{18}$$

where $d_k(\hat{\boldsymbol{x}}_{k|k-1})$ is the distance between the tracker's position $\boldsymbol{q}$ and the estimated position of the target $\hat{\boldsymbol{p}} = [\hat{p}_x, \hat{p}_y]^T = [\hat{\boldsymbol{x}}^x_{k|k-1}, \hat{\boldsymbol{x}}^y_{k|k-1}]^T$, $\boldsymbol{C}_k$ is the derivative of $d_k(\hat{\boldsymbol{x}}_{k|k-1})$ with respect to the state $\boldsymbol{x}$, $\boldsymbol{K}_k$ is the Kalman gain calculated on each update, $\hat{\boldsymbol{x}}_{k|k}$ is the state estimate after the update, $\boldsymbol{P}_{k|k}$ is the probability matrix after the update, and y_k is the registered range measurement of the real distance between the ASV tracker q and the AUV target p. The variance R is related to the noise associated with the range measurements $\eta_k \sim \mathcal{N}(0, R)$. A feature worth noting is when there is no new range measurement y_k, which translates in the Kalman gain $\boldsymbol{K}_k = \boldsymbol{0}$, which in turn means, in an intuitive way, that the state is equal to the predicted $\hat{\boldsymbol{x}}_{k|k} = \hat{\boldsymbol{x}}_{k|k-1}$, as well as the probability matrix $\boldsymbol{P}_{k|k} = \boldsymbol{P}_{k|k-1}$.

If the case of multiple range measurements is considered (multiple ASV trackers, for example), the system presented in Equation (18) changes slightly, where the measures $\boldsymbol{y}_k$, the distance $\boldsymbol{d}_k(\hat{\boldsymbol{x}}_{k|k-1})$ and the variance $\boldsymbol{R}$ are not scalars anymore, having the dimension corresponding to the number of range measurements. For instance, with two measures, $\boldsymbol{y}_k$ is 2×1, $\boldsymbol{d}_k(\hat{\boldsymbol{x}}_{k|k-1})$ is 2×1, taking into account that the position of the tracker $\boldsymbol{q}$ is dependent on the tracker which effectively performed the range measurement, $\boldsymbol{R}$ is 2×2, and $\boldsymbol{C}_k$ also changes and becomes 2×4.

3.6. Complementary Kalman Filter

The CKF is a Complementary Filter, such as the approach seen in [9], converted into a Kalman Filter so that time-varying gains are considered. The CKF is implemented in the AUV targets, since the underwater localisation problem is quite challenging. The filter receives the EKF estimates of the ASV tracker through the acoustic channel from time to time, and performs a correction on its estimated position based on the mounted DVL's velocity measurements. Therefore, the received EKF estimated position is treated as a sensor measurement. In Figure 6, the overall system can be observed.

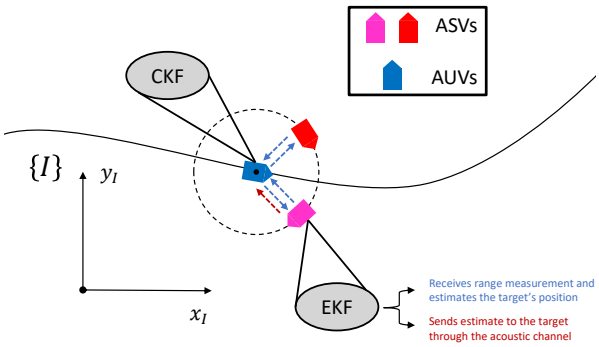

Figure 6: Illustration of the filter application.

From the Complementary Filter approach, the velocity measurements are considered a system input, and also a bias for currents is also taken into account. The state to be estimated is then given by $\boldsymbol{x} = [x, y, v_c^x, v_c^y]^T$, where $\boldsymbol{p} = [x, y]^T$ is the AUV target's position, and $\boldsymbol{v}_c = [v_c^x, v_c^y]^T$ is the current bias. The CKF prediction stage is defined as

$$\begin{cases} \hat{\boldsymbol{x}}_{k|k-1} = \boldsymbol{F} \cdot \hat{\boldsymbol{x}}_{k-1|k-1} + \boldsymbol{E} \cdot \boldsymbol{v}_k\,, \\ \boldsymbol{P}_{k|k-1} = \boldsymbol{F} \cdot \boldsymbol{P}_{k-1|k-1} \cdot \boldsymbol{F}^T + \boldsymbol{W}_\nu\,, \end{cases} \tag{19}$$

where

$$\boldsymbol{F} = T_s \cdot \begin{bmatrix} \boldsymbol{0} & \boldsymbol{I}_2 \\ \boldsymbol{0} & \boldsymbol{0} \end{bmatrix}, \quad \boldsymbol{E} = T_s \cdot \begin{bmatrix} \boldsymbol{I}_2 \\ \boldsymbol{0} \end{bmatrix}, \tag{20}$$

and $\boldsymbol{W}_\nu$ is the variance related to the process noise $\boldsymbol{w} \sim \mathcal{N}(0, \boldsymbol{W})$ and the velocity measurement input $\boldsymbol{v}_k$ noise $\boldsymbol{\nu} \sim \mathcal{N}(0, \boldsymbol{N})$. Since the two noises are independent, $\boldsymbol{W}_\nu$ is expressed as

$$\boldsymbol{W}_\nu = \boldsymbol{W} + \begin{bmatrix} \boldsymbol{N} & \boldsymbol{0} \\ \boldsymbol{0} & \boldsymbol{0} \end{bmatrix}. \tag{21}$$

Considering all this, the update stage is formulated as

$$\begin{cases} \boldsymbol{K}_k = \boldsymbol{P}_{k|k-1} \cdot \boldsymbol{C}^T (\boldsymbol{C} \cdot \boldsymbol{P}_{k|k-1} \cdot \boldsymbol{C}^T + \boldsymbol{P}_{EKF})^{-1}\,, \\ \hat{\boldsymbol{x}}_{k|k} = \hat{\boldsymbol{x}}_{k|k-1} + \boldsymbol{K}_k (\boldsymbol{p}_{EKF} - \boldsymbol{C} \cdot \boldsymbol{x})\,, \\ \boldsymbol{P}_{k|k} = (\boldsymbol{I}_4 - \boldsymbol{K}_k \cdot \boldsymbol{C}) \cdot \boldsymbol{P}_{k|k-1}\,, \end{cases} \tag{22}$$

where a few differences between this update stage and the one from the previous section are noticed. To begin with, the system is completely linear, with the output being calculated simply by multiplying the matrix $\boldsymbol{C}$ with the state vector $\boldsymbol{x}$. The probability matrix $\boldsymbol{P}_{EKF}$ is received from time to time

along with the EKF position estimation $\boldsymbol{p}_{EKF}$, to give a certainty of the value that is being calculated in the EKF implemented on the tracker ASVs.

3.7. Smart Cooperative Path Following

The velocity law of SCPF is designed to substitute the previously designed desired velocity law v_d in the CPF section, represented in (8), so that the vehicles focus solely on performing a simple PF technique with a certain velocity profile v_p before starting to correct their velocity with the correction term v_c in order to coordinate with their neighbours. Thus, a new desired velocity law is proposed for vehicle i as

$$v_d^{[i]} = v_p + \underbrace{(1 - \tanh(k_s \cdot e_f^{[i]}))}_{\text{convergence to path control}} \cdot v_c \,, \tag{23}$$

where v_p is the ordinarily assigned speed profile, v_c is the velocity correction associated with the CPF performance, and k_s is the sensitivity tuning parameter for the distance of the vehicle i to its virtual target on the path $e_f^{[i]}$, which in turn is defined by

$$e_f^{[i]} = ||\boldsymbol{p}^{[i]} - \boldsymbol{p}_s^{[i]}|| \,, \tag{24}$$

where $\boldsymbol{p}^{[i]}$ is the vehicle's position, and $\boldsymbol{p}_s^{[i]}$ the respective virtual target position on the path, previously determined by the PF algorithm. The fact that the SCPF focuses on reaching the path with PF techniques before performing CPF does even more justice to the assumption made on the normalisation of the virtual target s to determine the coordination state γ of the vehicle.

3.8. Cooperative Multiple Formation Control

The final step of the projected system is the CMFC, the cooperation between two different formations, a group of ASV trackers $\mathcal{F}_{ASV}$ and a group of AUV targets $\mathcal{F}_{AUV}$. For this, a new communication channel is defined between an elected AUV target from $\mathcal{F}_{AUV}$ and an elected ASV tracker from $\mathcal{F}_{ASV}$. Therefore, one resorts to the CPF/ETC strategies mentioned before, creating a new cooperation layer. Figure 7 shows the general idea of the proposed control mechanism.

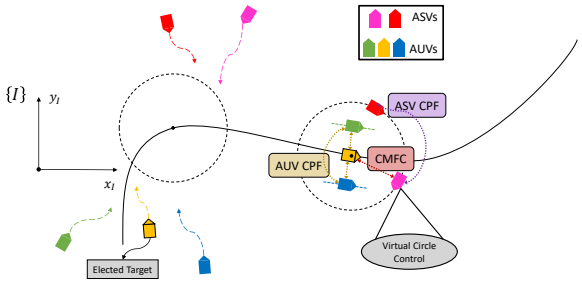

Figure 7: Illustration of the Cooperative Multiple Formation Control system.

To this end, a new coordination state is defined within the elected ASV tracker, dictating the position of the virtual circle created during the MPF design. The moving circle then shares its path with the elected target, although practically on different planes, the problem never leaves the 2D assumption, so the AUV target and the ASV tracker are considered on the same plane. Having this said, now the virtual circle can freely converge to the elected target, and vice versa, with the help of a newly designed velocity law for both the elected target and the virtual circle moving along the path. First, consider the average of the distances from the ASVs to their corresponding virtual targets s on their respective paths, given as

$$e_f^{av} = \frac{1}{|\mathcal{N}_{ASV}|} \sum_{m \in \mathcal{N}_{ASV}} e_f^{[m]} \,, \tag{25}$$

where $\mathcal{N}_{ASV}$ is the total number of ASV trackers circulating the moving path, and $e_f^{[m]}$ is the distance of the ASV m relative to its virtual target, determined in the previous section. The moving circular path is controlled to care for not only misalignment between its own coordination state and the elected AUV target's coordination state, but it also does not start moving along the path with the velocity profile v_p before the ASV trackers converge to the circular path. It is then governed by the velocity law defined as

$$v_{\odot} = \underbrace{(1 - \tanh(k_f \cdot e_f^{av}))}_{\text{vehicle distance to moving path control}} \cdot v_p + v_{cf} \,, \tag{26}$$

where k_f is a sensitivity tuning gain for the average of the distances from the ASVs to their corresponding virtual targets e_f^{av}. The velocity correction for the formation coordination control v_{cf} is always active and follows the classic CPF logic. Once the virtual circle is coordinated with the elected AUV target, the velocity correction v_{cf} converges to zero. The velocity correction for the formations is then

expressed as

$$v_{cf}^{[i]} = -k_{\xi f}^{[i]} \cdot \tanh\left(\gamma_i^{[i]} - \frac{1}{|\mathcal{N}_i|}\sum_{j\in\mathcal{N}_i}\hat{\gamma}_j^{[i]}\right), \quad (27)$$

where $k_{\xi f}^{[i]}$ is a tuning parameter for the convergence of coordination states between formations, determining the minimum and maximum values of the velocity correction of the formations v_{cf}, where i either corresponds to the elected AUV target or the virtual circle. The terms inside the hyperbolic tangent represent the difference between $\gamma_i^{[i]}$, the actual coordination state γ of i and the average of the estimates of the neighbour coordination states $\hat{\gamma}_j^{[i]}$.
The elected target must also be controlled in order to account for the new formation cooperation layer with the virtual circle projected within the elected ASV tracker. To this end, the velocity control law for the elected target is formulated as

$$v_{target} = v_p + \underbrace{(1 - \tanh(k_s \cdot e_f^{[target]}))}_{\text{SCPF}} \cdot (v_c + v_{cf}), \quad (28)$$

where the terms v_c and v_{cf} are the correction velocities computed in (9) and (27), respectively, and the SCPF term has already been discussed in the last section, as it is applied to every vehicle in the system.
The CMFC is now defined, though a new velocity control law is also defined to activate the trackers after they converge to the virtual circle and the elected AUV target becomes coordinated with the virtual circle. In other words, the ASV trackers remain fixed in relation with the moving path until the elected AUV target and the virtual circle itself become coordinated. Considering all this, an error between the two coordinated states is defined as

$$\gamma_{error} = \gamma_{\odot} - \hat{\gamma}_{target}, \quad (29)$$

where $\gamma_{\odot}$ is the coordination state of the virtual circle, and $\hat{\gamma}_{target}$ is the estimated coordination state of the elected AUV target, since the trackers do not have access to the target's state at all times. The designed velocity control law for the trackers is then defined as

$$\begin{aligned} v_{tracker} = (& \underbrace{1 - \tanh(k_g \cdot |\gamma_{error}|)}_{\text{formation discoordination control}} + \\ & + \underbrace{\tanh(k_s \cdot e_f^{[tracker]})}_{\text{compensation for SCPF}}) \cdot v_p + \\ & + \underbrace{(1 - \tanh(k_s \cdot e_f^{[tracker]}))}_{\text{SCPF}} \cdot v_c, \end{aligned} \quad (30)$$

where k_g is the sensitivity tuning parameter for the coordination state error γ_{error}, and v_c is the usual velocity correction of the CPF layer between the ASVs. The formation discoordination control is the term which gives the ASVs the ability to wait for the vehicle formations to align. A compensation term for the SCPF is implemented, so that the tracker moves even if it finds itself far from the virtual circle, since now there is no velocity correction while the ASV does not reach the moving path.

4. Simulation Results

The proposed system was accomplished and is reviewed in the next sections, taking into consideration the simulation results

4.1. Code Review

The system was iteratively implemented in python3, in a stack produced specifically for this work. It can be found in [11], with simulations regarding each step that leads to the final system. Each concept explained in this work was developed in a different module, so that it could be tested without the influence of the other subsystems. Moreover, in order to analyse the simulation results, a dashboard with plot of interest was implemented, with the possibility of having an animation of the mission as it is running.

4.2. Simulations

The final system is translated in a simulation composed of a formation of three AUV targets $\mathcal{F}_{AUV}$, with a local CPF strategy within the formation, which in turn cooperates with a similar ASV tracker formation $\mathcal{F}_{ASV}$ of two vehicles, since a local CPF strategy is also applied. The ASVs perform an encircling manoeuvre over an elected AUV target from $\mathcal{F}_{AUV}$ using MPF techniques. Moreover, a filter application like the ones seen in 3.5 and 3.6 is implemented on the system. The EKFs are implemented on the elected ASV tracker that performs range measurements to each AUV target in $\mathcal{F}_{AUV}$, and receives similar range measurements performed by the other ASV tracker. Each EKF estimate of the position of the AUV targets is then broadcasted to each of the vehicles in $\mathcal{F}_{AUV}$ so that a mounted CKF can blend that information with its estimate of its own position, helping to the underwater localisation of the AUVs. Considering all this, the acoustic channel between $\mathcal{F}_{ASV}$ and $\mathcal{F}_{AUV}$ encompass the range measurements, the transmission of the EKF estimate, and the coordination state of the virtual circle from the CMFC. The resulting system is represented in Figure 8, showing in a simplified manner how the CMFC works in tandem with the concepts explained in the previous sections.

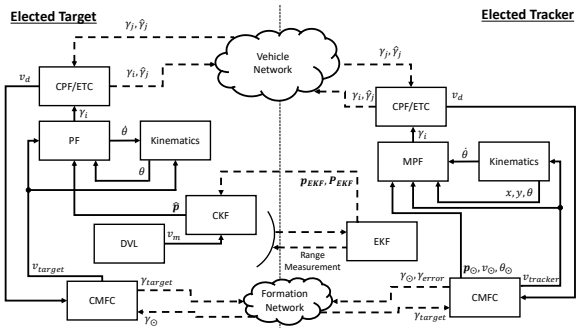

Figure 8: Cooperative Multiple Formation Control mechanism implemented on the overall system, represented in block diagram.

The transmission of the EKF estimates starts only after the error between the virtual circle and the elected AUV target is not greater than a certain maximum error threshold t_h. This mechanism shows better performance, since the EKF estimates have time to be better estimated as the vehicles converge to their respective paths. The threshold, for this simulation, was considered as $t_h = 0.05$.

The values for the parameters used during the simulation are displayed on Tables 1, 2, 3, 4 and in Equations (31) and (32).

Table 1: Path Following values.

γ	k_1	k_2	k_{delta}	θ_a
1	1	0.3	0.5	0.8

Table 2: Cooperative Path Following values.

AUV					
k_ξ^0	v_p^0	k_ξ^1	v_p^1	k_ξ^2	v_p^2
0.12	0.16	0.15	0.2	0.18	0.24

ASV			
k_ξ^0	v_p^0	k_ξ^1	v_p^1
0.4	0.5	0.4	0.5

Table 3: Event-Triggered Communications values.

c_0	c_1	c_2
0.01	0.5	1

For the EKF, the following variances were used

$$\boldsymbol{Q} = 10 \cdot e^{-6} \begin{bmatrix} 10 & 0 & 0 & 0 \\ 0 & 10 & 0 & 0 \\ 0 & 0 & 1 & 0 \\ 0 & 0 & 0 & 1 \end{bmatrix}, \boldsymbol{R} = \begin{bmatrix} 0.01 & 0 \\ 0 & 0.01 \end{bmatrix}. \tag{31}$$

For the CKF, the following variances were used

$$\boldsymbol{W} = 10 \cdot e^{-6} \begin{bmatrix} 10 & 0 & 0 & 0 \\ 0 & 10 & 0 & 0 \\ 0 & 0 & 1 & 0 \\ 0 & 0 & 0 & 1 \end{bmatrix}, \boldsymbol{N} = \begin{bmatrix} 0.1 & 0 \\ 0 & 0.1 \end{bmatrix}. \tag{32}$$

Table 4: Cooperative Multiple Formation Control and Smart Cooperative Path Following values.

$k_{\xi f}^{target}$	$k_{\xi f}^{\odot}$	k_f	k_g	k_s
0.1	0.1	1	0.1	0.01

The simulation shows the designed CMFC technique in action, as well as both filter applications. The Cooperative Formation Control plot presents the convergence between the elected AUV target coordination state γ_{target} and the coordination state $\gamma_\odot$ of the virtual circle projected within one the ASV trackers, as the two lines converge. The communications derived from the ETC mechanism are also visible, indicating that the two different formations $\mathcal{F}_{ASV}$ and $\mathcal{F}_{AUV}$ achieve coordination between each other. The Vehicle Position plot not only suggests that, but also demonstrates the good behaviour of the designed filters. The EKFs implemented on the elected ASV tracker estimate the position and velocity of the AUV targets, showing good performance on the EKF Error plot, where the distance between the estimates and the real positions of the AUV targets is minimal. This serves as a great launching point for the CKFs implemented on each AUV target, which performance is represented in the CKF Error plot. As observed, the distance between the CKFs' prediction for each target's position and the its actual position is also quite small. Thus, the velocities of all vehicles, including the virtual circle, converge to the velocity profile assigned to each path.

5. Conclusions

A cooperative system between distinct vehicle formations was proposed in the context of seismic surveying missions. A group of locally cooperative AUV targets and a group of locally cooperative ASV trackers worked together to achieve the desired ASV tracker encircling manoeuvre around the AUV targets. As seen in the simulations in the previous section, the objective was achieved, including

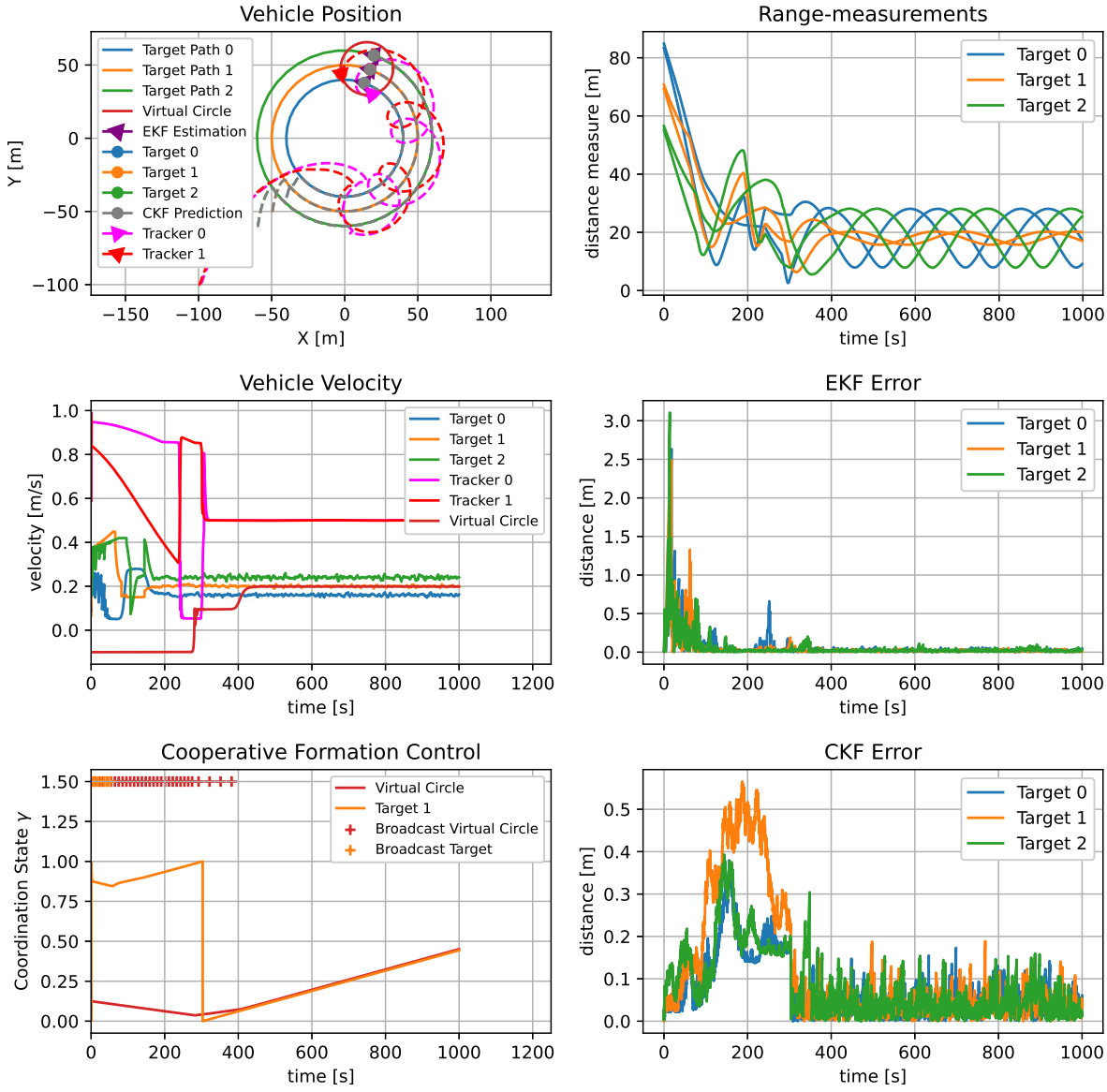

Figure 9: Plotting of the Cooperative Multiple Formation Control simulation result.

a filter application to accommodate the system to the constraints found in the real case. Even with a high variance on the DVL's velocity measurements, the CKF shows reasonable behaviour with the reception of the AUV EKF estimates from the ASV trackers.

5.1. Future Work

The next natural step would be to implement the system in the real case, with actual AUVs and ASVs to test the performance of the designed control algorithms. Althought the velocities are bounded and vehicle convergence to the path is assured, proof of stability and general mathematical coherence would also be a worthwhile study to backup even more the proposed system of CMFC.

Finally, its is suggested to explore the caveats of the mission at hand, where mechanisms to better ensure the malfunction of certain systems do not compromise the whole mission, like the temporary cessation of the range measurement readings for the EKF and the subsequent resuming of the mission.

Acknowledgements

This work was partially financed by the projects EU Marine Robotics Research Infrastructure Network [ID731103], and European Multidisciplinary Seafloor and Water Column Observatory (Portugal) [LISBOA-01-0145-FEDER-022157], through Institute for Systems and Robotics (ISR).

References

[1] G. Indiveri. Widely scalable Mobile Underwater Sonar Technology WiMUST Proposal. 2014.

[2] L. Lapierre, D. Soetanto, and A. Pascoal. Nonsingular path following control of a unicycle in the presence of parametric modelling uncertainties. *INTERNATIONAL JOURNAL OF ROBUST AND NONLINEAR CONTROL*, pages 485–503, April 2006.

[3] R. Ghabcheloo, A. P. Aguiar, A. Pascoal, C. Silvestre, I. Kaminer, and J. Hespanha. Coordinated path-following in the presence of communication losses and time delays. *SIAM - Journal on Control and Optimization, Vol. 48, No. 1*, pages 234–265, 2009.

[4] R. Rego, N. Hung, and A. Pascoal. Cooperative Motion Control Using Hybrid Acoustic-Optical Communication Networks. *IFAC-PapersOnLine*, 54(16): 232–237, 2021. ISSN 2405-8963. doi: https://doi.org/10.1016/j.ifacol.2021.10.098. URL `https://www.sciencedirect.com/science/article/pii/S2405896321015007`. 13th IFAC Conference on Control Applications in Marine Systems, Robotics, and Vehicles CAMS 2021.

[5] N. T. Hung, F. C. Rego, and A. M. Pascoal. Event-Triggered Communications for the Synchronization of Nonlinear Multi Agent Systems on Weight-Balanced Digraphs. In *2019 18th European Control Conference (ECC)*, pages 2713–2718, 2019. doi: 10.23919/ECC.2019.8796277.

[6] T. Oliveira, A. P. Aguiar, and P. Encarnação. Moving Path Following for Unmanned Aerial Vehicles with Applications to Single and Multiple Target Tracking Problems. *IEEE Transactions on Robotics, Vol. 32, Issue 5*, October 2016.

[7] D. Teixeira. Sensor-Based Cooperative Control of Multiple Autonomous Marine Vehicles. Master's thesis, Instituto Superior Técnico, Lisbon, October 2019. MSc in Electrical and Computer Engineering.

[8] N. T. Hung, F. F. C. Rego, and A. M. Pascoal. Cooperative Distributed Estimation and Control of Multiple Autonomous Vehicles for Range-Based Underwater Target Localization and Pursuit. *IEEE Transactions on Control Systems Technology*, pages 1–15, 2021. doi: 10.1109/TCST.2021.3107346.

[9] A. Pascoal, I. Kaminer, and P. Oliveira. Navigation system design using time-varying complementary filters. *IEEE Transactions on Aerospace and Electronic Systems*, 36(4):1099–1114, 2000. doi: 10.1109/7.892661.

[10] F. V. Vanni. Coordinated Motion Control of Multiple Autonomous Underwater Vehicles. Master's thesis, Instituto Superior Técnico, July 2007. MSc in Aerospace Engineering.

[11] F. Branco. Github Thesis Repository: Cooperative Marine Vehicle Navigation and Control with Applications to Geotechnical Surveying. https://github.com/franciscobranco/Thesis.